machines

MDPI

Article

Modular Design and Layout Planning of Tooling Structures for Aircraft Assembly

Zhanghu Shi [1,2], Chengyu Li [1], Junshan Hu [1,*], Xingtao Su [1], Hancheng Wang [1] and Wei Tian [1]

[1] College of Mechanical and Electrical Engineering, Nanjing University of Aeronautics and Astronautics, Nanjing 210016, China
[2] Aviation Industry Chengdu Aircraft Industry (Group) Co., Ltd., Chengdu 610092, China
* Correspondence: hujunshan@nuaa.edu.cn; Tel.: +86-159-5168-3586

Abstract: Aircraft structures consist of numerous complex components that require a high level of precision to assemble. Tooling plays a crucial role in the assembly of aircraft components, providing the functions of positioning, shape maintenance, and support to guarantee the accuracy of the product. Aiming to obtain reusable assembly tooling that can be rapidly reconfigured, this study focuses on the modular design and layout of tooling structures. The concept of functional elements for the characterization of tooling parts is proposed, and the relationship between each pair of elements is established to clarify the similarities and dependencies among various tooling structures. Based on the analysis of functional elements and their relationships, the tooling structures are divided and recombined into several modules. The detailed module designs are demonstrated by using typical structures such as platforms, columns, and locators as examples. A parametric representation of the multi-source information of tooling modules is proposed, and optimization methods for the layout and configuration of locators and platforms are developed using their parametric information. A reconfigurable tooling process integrated with a monitoring system is designed, realized, and successfully applied to the assembly of a practical type of fuselage. The results from verifying these methods' efficiencies show that the modular design and reconfiguration planning of tooling only takes about 10 min and a few seconds, respectively, which is far less than the time consumed during traditional tooling design (from several days to weeks). The work in this study provides an engineering paradigm for the serialization and reconfiguration of assembly tooling in aviation manufacturing.

Keywords: aircraft assembly; reconfigurable tooling; modular design; layout planning

check for updates

Academic Editors: Feiyan Guo and Zhengping Chang

Received: 10 January 2025
Revised: 13 February 2025
Accepted: 20 February 2025
Published: 25 February 2025

Citation: Shi, Z.; Li, C.; Hu, J.; Su, X.; Wang, H.; Tian, W. Modular Design and Layout Planning of Tooling Structures for Aircraft Assembly. *Machines* **2025**, *13*, 185. https://doi.org/10.3390/machines13030185

Copyright: © 2025 by the authors. Licensee MDPI, Basel, Switzerland. This article is an open access article distributed under the terms and conditions of the Creative Commons Attribution (CC BY) license (https://creativecommons.org/licenses/by/4.0/).

1. Introduction

There are numerous structural components to an aircraft that are diverse and have high requirements for precision assembly [1]. In the assembly process, tooling provides functions including positioning, shape maintenance, and fixed support for aircraft components [1,2]. Traditional assembly tooling is mostly made of robust steel parts that are permanently welded together to ensure the structural rigidity and stability required for accurate positioning. These positioning and supporting parts are densely arranged and are typically used for a specific aircraft product. This tooling design scheme results in poor openness of the assembly space and means that the tooling cannot be reused when the product is changed. Thus, it is difficult to adjust to a manufacturing mode that can realize the small-batch production of multiple varieties in the future. While ensuring structural stability is important, investigating the modularization and reconfigurability of the tooling

process is also beneficial for enabling a rapid response to product change and assessing the efficiency of tooling usage.

Focusing on the reconfigurability and adaptability of assembly tooling, aviation enterprises around the world have conducted considerable research on digital measurement and control technologies. For instance, various types of reconfigurable tooling have been developed; these are also known as flexible tooling and can be configured according to different assembly tasks. The currently used flexible tooling can be classified into three types: high-speed column tooling [1,3], multi-point forming tooling [1,4], and positioning tooling based on parallel mechanisms [1,5]. High-speed column tooling is mainly used to position and support slender parts, such as wing beams and stringers; multi-point forming tooling is suitable for the shaping and single-coordinate positioning of thin-walled parts, and flexible tooling based on parallel mechanisms is used for the posture alignment of large components. Bojite developed two types of tooling, the Eco Positioner and Flexible Section Assembly Cell, which have been applied to fuselage positioning in Boeing and Airbus aircraft assemblies [1,6]. Shanghai Aircraft Manufacturing applied the Eco Positioner to the automated fuselage assembly of the C919 [1,7]. Ke et al. [8] have developed an attitude adjustment system for fuselage, improving the quality and efficiency of aircraft assembly through numerical control locators. Huang et al. [9] used a parallel mechanism based on numerical control locators for the assembly of fuselage and wings. Li et al. [1,10] have developed a monitoring system for detecting the positioning error and clamping force of a type of assembly tooling that can be reconfigured for different fuselages. Muller et al. [1,11] have developed a reconfigurable tooling based on parallel mechanisms for the assembly of fuselage walls. Thomas et al. [1,12] realized the modularization of parallel mechanisms for adaptation to various types of assembly parts. The above types of tooling have some adaptability to the assembly of different products. However, their current design still relies on human experience, and there is no unified standard or routinized process for their design. The development process of tooling is time-consuming, and its adaptation to various products is limited.

Aiming to achieve the goal of a standardized design, some institutions have integrated modular structures with reconfigurable technologies and proposed the concept of low-cost reconfigurable tooling based on box connections [1,13]. This type of tooling incorporates all of the modular parts, including the main frame, the mechanisms for positioning, the connection structures, and measurement devices. The overall structure of this tooling is adjustable and detachable, which can significantly improve the utilization rate of assembly tooling resources [1,14,15]. Löchte [1,16] proposed a six-SPS parallel mechanism to achieve adjustment through the reconfigurable connection of parallel mechanism branches. Prause [1,17] developed a three-PUU parallel mechanism for the positioning of fuselage panels during assembly and obtained an optimized bearing capability through the reconfiguration of parallel mechanism branches. Saab and Linkoping University have proposed the concept of Affordable Reconfigurable Tooling (ART) [1,13,18], which uses a series of modular mechanisms and effectively reduces the precision requirements for installation, thereby saving costs. It was successfully applied to the assembly of the "Neuron" unmanned aerial vehicle [1,19]. In 2009, Saab and Airbus established the first box-joint tooling based on the ART concept and successfully applied it to the assembly of wing boxes [1,20]. Considering that ART adopts an offline reconfiguration strategy that cannot realize the posture adjustment of aircraft components, some reconfigurable tooling systems have been developed using a combination of servo control and modular structures to improve their adaptability. Xiong [1,21] proposed a tooling system consisting of a mobile base, parallel mechanisms, and clamping mechanisms for the capability of online reconfiguration. Mannheim [1,22] developed a flexible gripper that can automatically reconfigure itself by

adjusting the configuration of parallel mechanisms in real time. Molfino [1,23] developed an assembly platform called SwarmItFIX that can automatically adjust its positioning units online, and it was successfully applied in clamping and holding processes. The Airbus company proposed a flexible assembly system called FAHF [1,24] that can respond to customer needs in a timely manner and has a lower cost. Francesco et al. [1,14] developed an automated synthesis of multiple robotic cells on reconfigurable tooling to realize the cooperation thereof for aircraft assembly, and they validated this in the European LOCOMACHS (Low-Cost Manufacturing and Assembly of Composite and Hybrid Structures) project. Based on this project, Ilker et al. [1,25] also presented a framework for automated flexible tooling development and presented their results on a hexapod fixture as a case study.

In summary, focusing on the reconfigurability, adaptability, and low-cost design of aircraft assembly tooling, considerable research has been conducted on digital measurement, mechanism design, and servo control in academia and industry, and various types of flexible tooling have been developed. However, the modular design of reconfigurable tooling lacks a general guiding framework, and the degrees of modularization and serialization of tooling structures are still insufficient. Moreover, in order to improve the adaptability and reconfigurability of tooling, a large number of studies focus on online measurement and servo control while neglecting the importance of rigidity and stability. The application of a multiple-degree-of-freedom mechanism driven by a servo motor makes it impossible for reconfigurable tooling to have adequate rigidity and repeatable accuracy of positioning. An automated servo system is indeed useless for the assembly of small parts, since the parts can be placed and fixed on tooling rapidly and manually by workers. So, there is a demand for attention to the development of assembly tooling that is reconfigured using some releasable structures, as this would have more application prospects for the assembly of small parts due to both its stiffness and its adaptability.

Therefore, this study focuses on a general framework of structural design and rapid reconfiguration for tooling that is configured using releasable connections and is used in the assembly of small parts. A modular design theory based on the concept of functional elements and a planning method for reconfiguration based on optimization algorithms are proposed. Through the analysis of so-called functional elements, the differences and similarities between various structures of the tooling are clarified, and the structures are reorganized and divided into several modules. A parametric representation and a storage strategy for the design information of modules are proposed. Depending on the parametric information, the layouts of two typical structures, namely, a locator and platform, are optimized to realize the rapid reconfiguration of tooling. It is hoped that these works can provide a paradigm for the serialization and modularization of assembly tooling. The main contributions of this study are as follows:

(1) The first contribution is the modularization and routinized design of assembly tooling structures that have both adaptability and rigidity. Unlike reconfigurable tooling based on a servo mechanism, the type of tooling developed in this study is reconfigured with releasable connections and is more applicable due to its structural robustness and the stability of its accuracy. Benefiting from reasonable classification and reorganization of mechanical structures, the modularization and rapid design of assembly tooling, which are neglected by academics but need more attention in engineering, are realized in this study.

(2) The second contribution is the planning of the layout of assembly tooling structures. Based on the robust and adaptable tooling developed, the authors propose two intelligent planning algorithms for the layouts of platform units and locating points to enhance the efficiency and automation of configuration. The efficient plan-

ning of reconfiguration further enhances the adaptability and usage of this tooling in engineering.

2. Modular Design Method for Tooling Based on Functional Elements

2.1. Problem Configuration

Traditional assembly tooling mainly consists of a main frame and functional parts, including positioning and clamping components, as shown in Figure 1a. The main frame is highly rigid, supporting the entire tooling structure and ensuring the positional stability of numerous locators and clamps, which are in direct contact with the aircraft product. In order to guarantee the positioning accuracy and support for the aircraft product, the locators and clamps are densely distributed and permanently fixed to the main frame, resulting in poor openness of the assembly space and weak adjustability. Therefore, this study aims to develop a type of tooling that uses reconfigurable locators and supports that are lightweight and low in density, as shown in Figure 1b. The reconfigurable tooling mainly consists of a platform, columns, cantilever locators, and auxiliary clamps. These structures are all connected through detachable bolts or movable slides, allowing the tooling's layout to be changed according to the product. Compared with the types based on servo mechanisms, this reconfigurable tooling is adaptable while retaining adequate rigidity and stability; thus, it has more applications in practice.

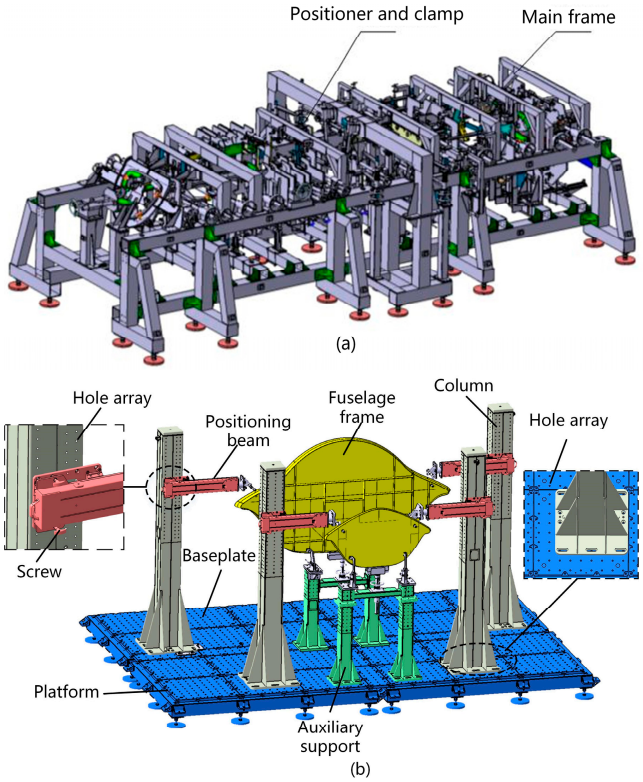


Figure 1. (**a**) Traditional rigid tooling in cage form; (**b**) modular and reconfigurable tooling developed in this study.

Although the new generation of tooling improves the openness of the assembly space and the reusability of the structure, there is still a lack of a general framework for the routinized design of tooling. Designs have relied on human experience so far and are time-consuming. Moreover, when a product is modified, the reconfiguration scheme lacks a fast and efficient optimization strategy, thus limiting the speed of response to the assembly tasks. This study draws attention to the general design method and rapid layout technology for

reconfigurable tooling. Based on the analysis of similarities between the functions of parts, tooling structures are divided and reorganized into several modules, forming a routinized and general design paradigm. For the purpose of rapid reconfiguration, a parametric representation of structural information and optimization algorithms for layout planning are proposed.

2.2. Functional Element Analysis and Modular Division of Tooling

For the convenience of functional analysis, the *i* th function of tooling is defined as FR_i, and a tree diagram is used to clarify the relationships between multiple functions provided by the assembly tooling from top to bottom, as shown in Figure 2. A function may be composed of multiple subfunctions that can be separately realized by different parts of the tooling, and the common function from which these subfunctions are derived is called their parent function. The functions are decomposed stage by stage until each subfunction can be implemented by an independent structure of the tooling. The subfunction located at the end of each branch in the diagram is called as a functional element and is marked in red in Figure 2. This figure gives an example of such a decomposition, where the functional elements are FR_4, FR_6, FR_8, FR_{10}, and FR_{11}~FR_{17}, and marked in red.

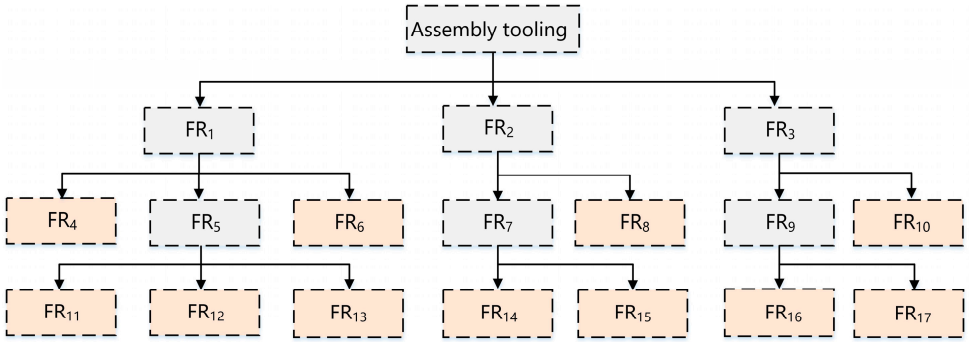


Figure 2. An example of the relationships between functional elements of assembly tooling.

We denote the distances from the functional elements FR_i and FR_j to their nearest common parent function as l_i and l_j, respectively; then, the relevance between FR_i and FR_j is defined as the following:

$$r(FR_i, FR_j) = r(FR_j, FR_i) = \begin{cases} x & x \geq 0.25 \\ 0 & x < 0.25 \end{cases}, \; x = \frac{1}{2^{l_i + l_j - 2}} \tag{1}$$

where $r(FR_i, FR_j)$ is the relevance between FR_i and FR_j, and l_i and l_j are the stages of distances between FR_i, FR_j, and their nearest common parent function. Based on the combination of the relatedness of each pair of functional elements, the following relevance matrix is defined as the following:

$$\boldsymbol{T} = \{r_{ij}\}_{n \times n} = \begin{bmatrix} r_{11} & r_{12} & \cdots & r_{1n} \\ r_{21} & r_{22} & \cdots & r_{2n} \\ \vdots & \vdots & \ddots & \vdots \\ r_{n1} & r_{n2} & \cdots & r_{nn} \end{bmatrix} \tag{2}$$

where $r_{ij} = r(FR_i, FR_j)$ is the relevance between FR_i and FR_j, and n is the total number of functional elements. Taking FR_6 and FR_{12} in Figure 2 as an example for calculation, their nearest common parent function is FR_1; then, $l_6 = 1$, $l_{12} = 2$, and, thus, $r_{6,12} = r(FR_6, FR_{12}) = 0.5$.

Based on the relevance matrix of functional elements, a binary matrix can be obtained by setting a threshold for the relevancies. This matrix represents a binary judgment of the similarity between each pair of functional elements. For example, if the threshold is

taken as λ, then the corresponding binary matrix ${}^{*}\boldsymbol{T}$ is shown in Equation (3), which can be expressed as the following:

$$ {}^{*}\boldsymbol{T} = \{t_{ij}\}_{n\times n},\ t_{ij} = \begin{cases} 1\ r_{ij} \geq \lambda \\ 0\ r_{ij} < \lambda \end{cases} \tag{3} $$

Based on the binary matrix ${}^{*}\boldsymbol{T}$ of functional element relevance, multiple similar elements are integrated into an entirety accordingly. In the matrix ${}^{*}\boldsymbol{T}$, if $t_{ij} = t_{i+1,\,j} = t_{i+2,\,j} = \ldots = t_{i+k,\,j} = 1$, then it is considered that the functions of FR_i, FR_{i+1}, … FR_{i+k}, FR_j are approximately equivalent. These functional elements are integrated into a new single element denoted as M_i, and their corresponding tooling structures are combined into a single module. Taking the original diagram of the functional elements in Figure 2 as an example, if the relevance threshold is $\lambda = 0.5$, the result of module division is shown in Figure 3, where the functional elements are reorganized into three modules denoted as M_1, M_2, and M_3.

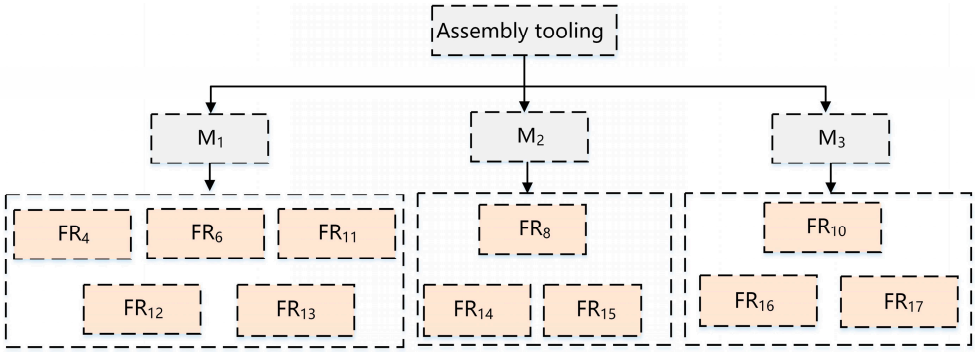


Figure 3. The division and integration of functional elements into modules.

2.3. Design Methods of Typical Modular Structures

As can be seen from the example of the reconfigurable assembly tooling shown in Figure 1, the typical modular structures of the tooling mainly include support platforms, columns, and locators. In this section, detailed structural design methods for these three typical types of modules are proposed.

2.3.1. Design of the Support Platform

The platform is used for the support of the whole structure of the assembly tooling and serves as a reference for installation. Unlike traditional tooling, which is fixed on the ground, the platform of the reconfigurable tooling provides adjustment capabilities for the structures installed on it. The platform has an array of bolt holes for the connections between itself and the tooling structures, allowing them to be moved conveniently. The platform is a combination of multiple units, and its total size depends on the maximum size of the working space envelope, which further depends on the maximum size of the product envelope according to the reference posture and top view, as well as the requirement for openness. The boundary of the platform should be greater than or equal to the boundary of the working space from the top view during assembly. Considering that various products have different requirements for the platform size, this study aims to meet these requirements to cover all types of products while using as few platform units as possible, thus saving time and supplies. Therefore, the platform is divided into units with a size of $l \times w$, such that a single-unit module can cover the envelope of the smallest products, and multiple units can be combined to meet the assembly requirements for the largest ones, as shown in Figure 4a.

According to the geometric relationship shown in Figure 4a, the boundary size condition of the platform can be expressed as the following:

$$\begin{cases} n_1 l \le L + a \\ n_2 w \le W + a \end{cases} \tag{4}$$

where n_1 is the number of units divided along the length direction, n_2 is the number of units divided along the width direction, and a is an experience value, which is usually taken as 700 mm.

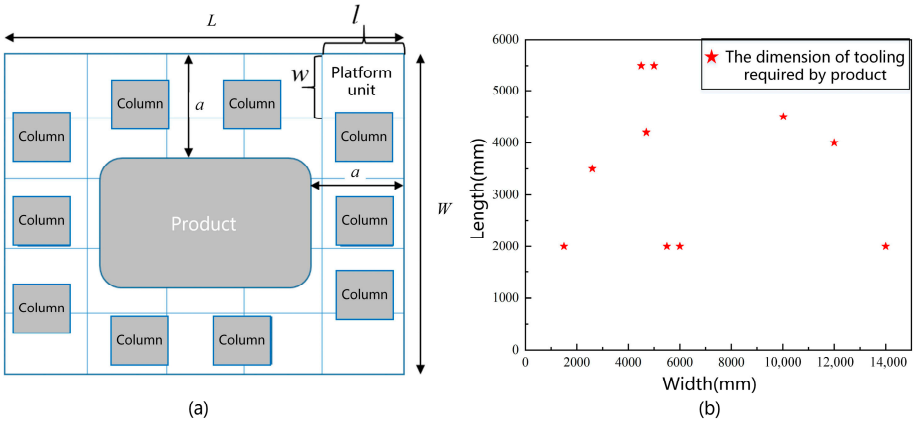


Figure 4. (**a**) Division and layout of the platform units; (**b**) statistics of the boundary sizes in product requirements.

By statistically analyzing the requirements for assembly space from 10 types of aircraft products, as shown in Figure 4b, the width direction is greater than or equal to 2000 mm. The greatest common divisor of all types of products from the top view is calculated, and the dimensions of the units are determined to be 3 m × 2 m after rounding, i.e., l = 3000 mm, w = 2000 mm.

In most cases, the platform is composed of two or more units, and the platform influences the horizontal accuracy of the structures installed on it. So, it must be possible for the posture of the platform to be adjusted. Regarding this requirement, this study further carries out modular and series designs of a matching surface, installation ports, and the integration of a leveling function, as shown in Figure 5. A single 3 m × 2 m platform unit consists of a mounting plate, support frame, leveling bolts, and other splicing parts, which are integrated and packaged. The mounting plate is drilled with a series of threaded holes in intervals of 100 mm, with a specification of M16 bolts. The parts of a single unit are fixed by splicing parts and finished bolts, and multiple units are attached by connecting plates and sockets to form an entire platform. In order to ensure the universality and interchangeability of the above parts, all dimensions and installation interfaces are designed with uniform specifications.

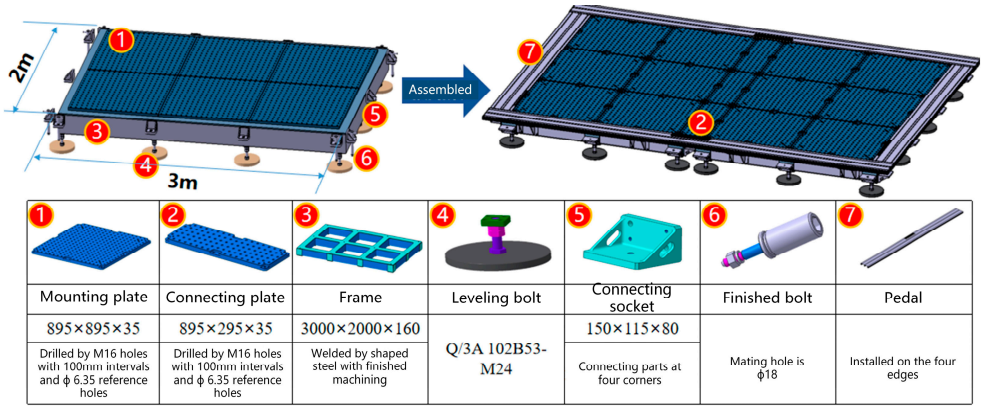


Figure 5. Design and combination of the platform unit.

2.3.2. Design of the Column Structure

The columns of the tooling are used for the installation of locators and clamps, and they act as the skeleton of the assembly tooling. Unlike the skeleton structure of traditional tooling, which is in a closed and welded form, the columns are distributed dispersedly in an open form in the design in this study. According to the requirements of the assembly process, the columns are located on both sides and the bottom of the product, and their sizes are determined by the height of the product in the assembly posture, as shown in Figure 6. The maximum envelope principle is used to determine the column specifications, and the columns are designed in series, producing six types of modules with heights of 5 m, 3 m, 1.1 m, 0.6 m, 0.4 m, and 0.2 m.

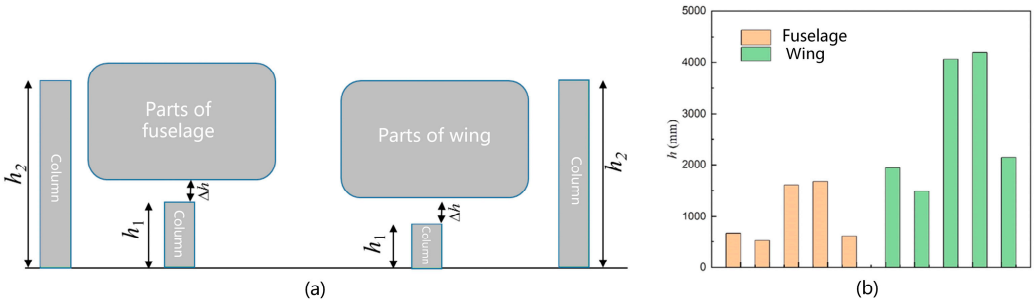


Figure 6. (**a**) Relationship between the column height and product size; (**b**) statistics of heights of multiple products.

Figure 7 shows the designed series of column modules. The bottom of a column is an installation interface that is in contact with the platform and is arranged with bolt holes. Because of the interchangeable design, the bolt holes have a diameter of 18 mm, and the distance between them is in multiples of 50 mm. Considering the rigidity of the column, a reinforcing rib is designed between the bottom and the column body. To provide a universal design, the column body is drilled with an array of screw holes for the installation of locators in different positions. In order to ensure the positioning accuracy of the locators, the flatness tolerance of the column plane does not exceed 0.1 mm, and its roughness is less than or equal to 1.6 μm. Considering the requirement for digital measurement during installation, placement holes for measurement targets for laser trackers are drilled on the top of the columns.

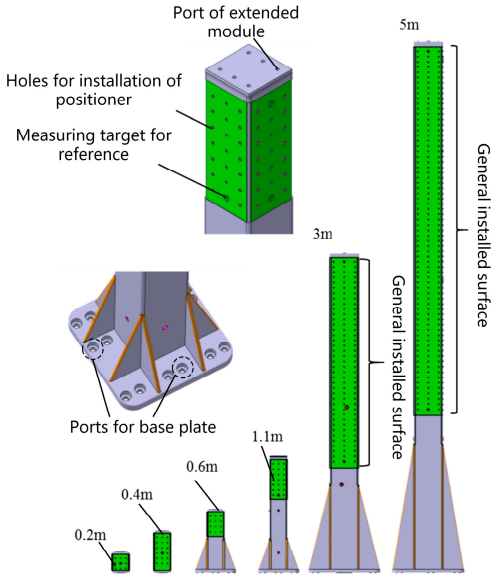


Figure 7. Design of the column structure in the tooling.

2.3.3. Locator Design

Locators are used for the precise positioning of products and provide some support functions for them. The modular structure of a locator mainly consists of three parts, namely, a beam, socket, and end effector. Each part has multiple types of modules, as shown in Figure 8a. Since the socket and end effector of a locator are in direct contact with the product and are designed according to the product, this study only carries out the modular design of the beam to achieve the maximum reuse rate of the structure. According to the structural form and usage requirements, the beams can be classified into two separate types based on sliding rails and guide posts. Guide post beams are often used when they are in contact with the product on the top of the post and can be further classified into two types based on whether they have a single guide post or double guide post. A single guide post is suitable for narrow spaces and is used as a support rather than a positioner due to its low rigidity. A double guide post is suited for the requirements of rigidity and positioning accuracy, such as when a product hole is being positioned after precision machining. Sliding rail beams are attached to the columns and can be classified into two types: single rails and double rails. The single rail type is only used in cases where the assembly space is narrow. In order to ensure guidance accuracy and rigidity, the scheme of double rails is generally adopted. According to actual requirements, a locator does not need to contain all three parts and can be classified into three types according to the combination of the parts. The first type consists of a beam, socket, and end effector; the second type consists of a beam and end effector; and the third type consists of a socket and end effector, as shown in Figure 8b. Considering that the double-sliding-rail beam is the most commonly used type of module in locators, this study only elaborates on the series design of this type of module.

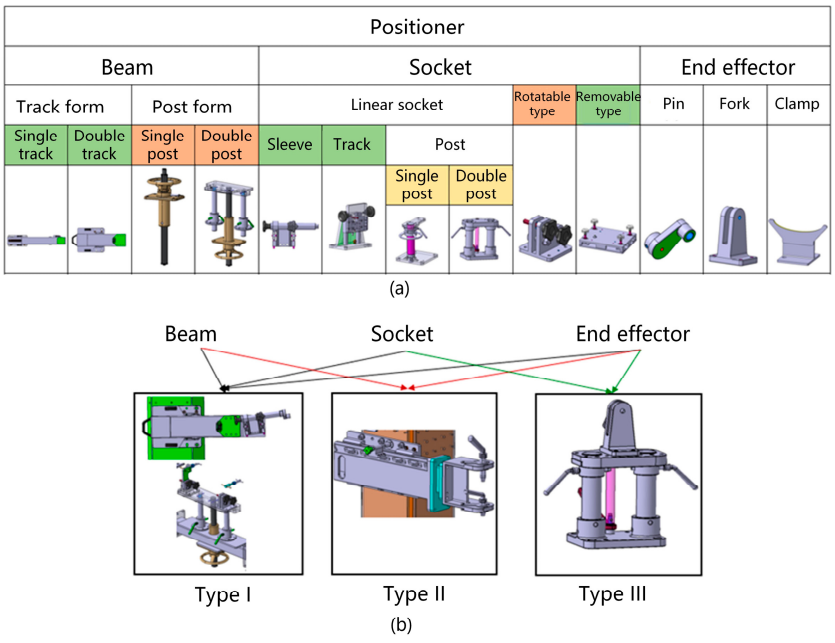


Figure 8. (**a**) Classification of the locator parts; (**b**) three types of modular locators.

Figure 9 shows the series design of a double-sliding-rail beam. According to the statistical data of the beam length required for usage, the beam can be classified into six specifications according to the different cantilever lengths, namely, 450 mm, 800 mm, 1000 mm, 1200 mm, 1400 mm, and 1600 mm, corresponding to different suspension demands. Each specification adopts the same structural form as that of the installation plate that is connected to the columns, is drilled with Φ18 mm through-holes, and is placed on

a sliding block in contact with the rail. The sliding rail provides mobility for the beam to adapt to different products and assembly spaces. The beam can be in two states: the working state and non-working state. When the product is placed on or off the tooling, the beam slides into the non-working state to make room for openness, and the beam enters the working state to meet positioning requirements during assembly. A locking pin is also integrated into the beam; this is used to ensure the stability of the tooling in different states. In addition, it also involves some holes for the placement of measurement targets used during digital installation and accuracy evaluation.

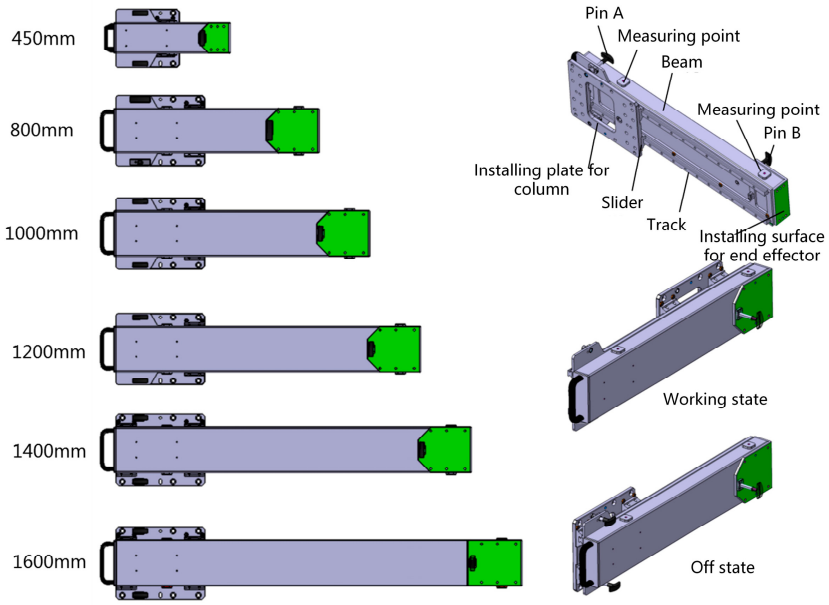


Figure 9. Series design of the locator arms based on a double sliding rail.

3. Optimization of the Layout of Reconfigurable Tooling Modules

On the basis of the modular design of the tooling structure, quickly configuring each functional module and guaranteeing the positioning and support while achieving the simplification of the tooling structure are the keys to the rapid response to product modifications and efficient completion of assembly tasks. The efficient layout of positioning points and the rapid paving of platform units are the two main tasks in the reconfiguration process of modular tooling. This section focuses on researching intelligent planning technology to achieve rapid decision making and the optimization of tooling reconfiguration schemes.

3.1. Parametric Representation and Storage of Modular Structural Information

The modular structures of tooling and assembly products have contact constraints, geometric shapes, and other multi-source features. Achieving a parametric representation and the efficient storage of their information is the basis for intelligent reconfiguration planning. Therefore, this section first defines a modular unit symbol and product assembly symbol for the digital models of tooling and products. The modular unit symbol (*MUS*) is a set that parametrically represents the geometric characteristics, processing requirements, and executable functions of tooling modules and is banded with digital models, as shown in Equation (5), which can be expressed as the following:

$$MUS = \left\{ A_{Typ}^{Fea}, S_c, T_c, T_f \right\} \tag{5}$$

where A_{Typ}^{Fea} is the identifier of functions, including positioning, clamping, and support. Since a single module may have multiple functions, this identifier is defined as a 0–1 binary

vector containing three elements, each of which separately represents whether the module has one of the above three functions. S_c represents the roughness requirement of the module surface, including a rough surface, semi-finished surface, and finished surface. In general, the roughness requirements of various surfaces of a single module are consistent, so this identifier is defined as an integer variable with a range of -1, 0, 1. T_c is the type of contact between the module and the product, and it includes no contact, point contact, line contact, and surface contact. Considering that a single module generally has only one type of contact with the product, this identifier is also defined as an integer variable from -2 to 2. T_f is the type of assembly scene applicable to the module, such as fuselage skeleton assembly, automatic drilling, and the riveting of panels. It is defined as a 0–1 binary vector where each element represents the applicability of the module to a certain scene, where 0 indicates inapplicability and 1 indicates applicability.

The product assembly symbol (*PAS*) is defined for the digital model of the product, and it maps the function identifiers of all tooling modules to the corresponding sum of constraint points, the constraint surface normal, and the positioning, clamping, and support functions. It is defined using Equation (6). Equation (6) can be expressed as the following:

$$PAS = \left\{ F_{Poi}, D_{Fea}, \sum_{i=1}^{n} \left(A_{Typ}^{Fea} \right)_i \right\} \tag{6}$$

where $\boldsymbol{F}_{Poi}$ is a $3 \times n$ matrix representing the coordinate set of multiple constraint points between the tooling and the product. $\boldsymbol{D}_{Fea}$ is also a $3 \times n$ matrix representing the unit normal set of multiple constraint surfaces between the tooling and the product. $\sum_{i=1}^{n} \left(A_{Typ}^{Fea} \right)_i$ represents the sum of the binary vector of functions corresponding to each module. The modular unit identifier MUS has some limiting conditions that are determined by the designer according to experience and product models; it usually requires that the constraint points cannot be on the same line, and the number of modules with positioning functions cannot exceed three.

The composition of reconfigurable tooling is complex, as there are many types of structures. Therefore, based on the modular unit symbol of the tooling, a knowledge base for reconfigurable tooling design is established to manage the modules and facilitate the update and iteration of subsequent versions of structures. The process of designing the knowledge base is shown in Figure 10a. Firstly, the assembly tooling is divided into functional modules according to the method proposed in Section 2.2. Then, the design information of each module in the tooling and the product information are, respectively, converted into the MUS and PAS, as shown in Equations (5) and (6), and a database containing these symbols is established. Finally, by combining the database with prior knowledge of the assembly process, a mapping from the parameters of the PAS to the parameters of the MUS is established to build a knowledge base that associates the product information with the tooling structures. The knowledge base allows the sharing of various standard resources needed for rapid design and lays the foundation for the efficient planning of reconfiguration. The composition and architecture of the knowledge base are shown in Figure 10b, including the libraries of instances, rules, and parametric information. The instance library is composed of digital models of tooling modules that cover their geometric information, the rule library contains information on the constraints of connections and layouts between structures, and the parametric information library mainly consists of the MUSs corresponding to modules.

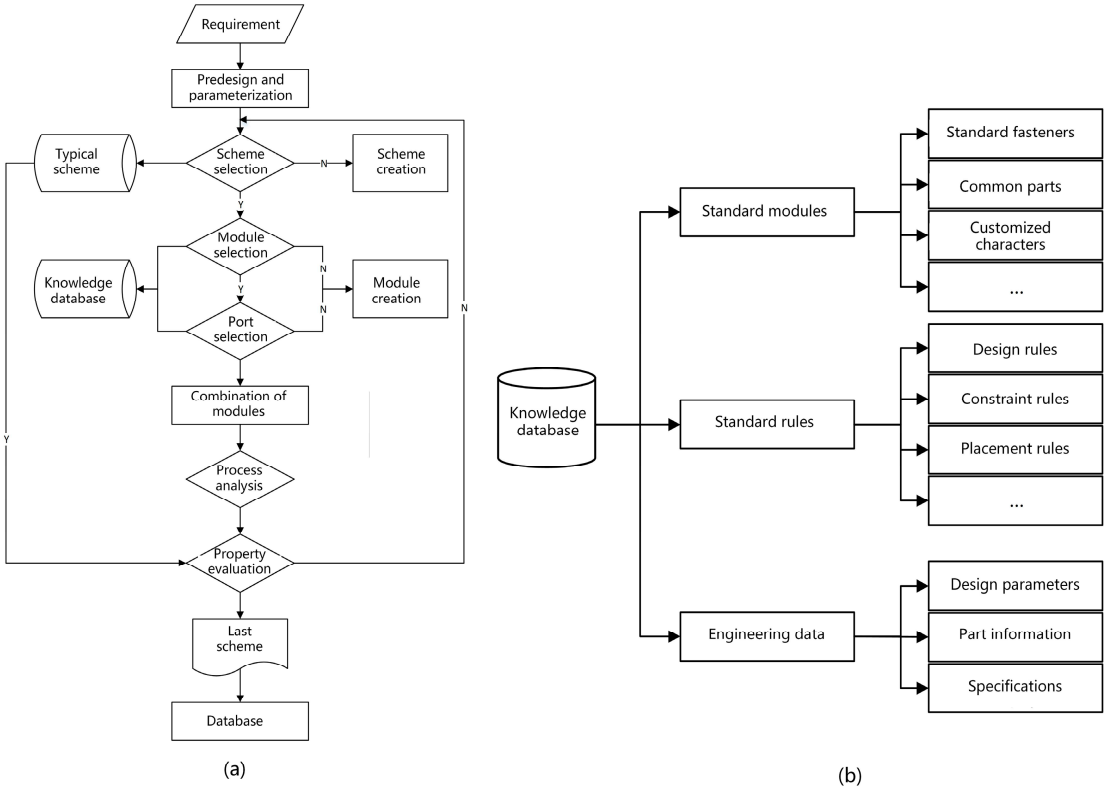


Figure 10. (**a**) Design process of the knowledge base for modular structures; (**b**) architecture of the knowledge base.

3.2. Layout Planning for Locators

In order to improve the degree of automation in the planning of the locator layout according to the product, this study proposes a locator planning method based on the DTW (Dynamic Time Warping) trajectory comparison algorithm using the parametric representation of the tooling structure. Different types of aircraft product components are classified, and their outer contours are simplified. The DTW algorithm can align two sequences of different lengths in time and can compare the similarities between them. The planning process for the locator layout based on the DTW algorithm consists of the following seven steps:

(1) Obtaining curve C_1: The outer contour curve C_1 of the aircraft component projected on the support platform of the tooling is extracted, and the smallest rectangle with size a that can envelop the curve C_1 on the platform plane is obtained. Then, a local coordinate system xoy is created, where the original point o is located at the midpoint of the rectangle, and the x and y axes are in the plane, as shown in Figure 11. Furthermore, the posture matrix T of the local coordinate system xoy relative to the aircraft coordinate system is obtained.

(2) Obtaining curve C_2: The typical positioning layouts suitable for the product in the knowledge base are projected onto the platform plane with the matrix $\boldsymbol{T}$, and the projected contour curve and the points of positioning location are extracted. The smallest rectangle enveloping the projected contour is created, and its length a′ is obtained in the same way as in step (1); then, a local coordinate system x′o′y′ is created. In order to facilitate subsequent trajectory comparisons, the projections of the contour curve and the location points are scaled with reference to the origin point o′, separately outputting curve C_2 and point set Z. The scaling ratio is a′/a. Then, the nearest point on C_2 corresponding to each of the points in Z is obtained, and these are

combined into a point set Y while recording the translation vectors from the points in Y to the corresponding points in Z.

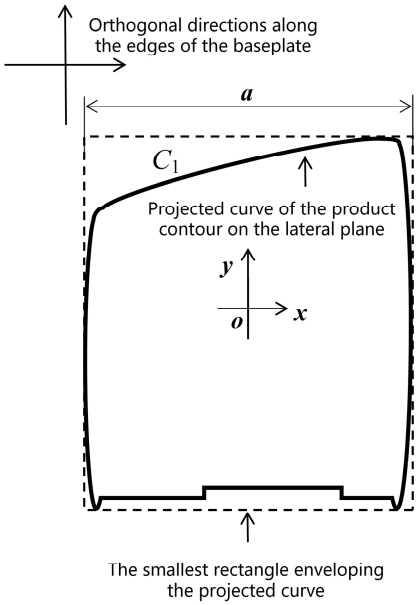


Figure 11. The projection of aircraft components on the supporting platform.

(3) Obtaining point sequences Q_1 and Q_2: The curve C_1 is discretized to obtain its point sequence Q_1, and the curve C_2 is discretized into points that are combined with the points in set Y to create sequence Q_2. The lengths of sequences Q_1 and Q_2 are denoted as n and m, respectively, as shown in Equation (7). Equation (7) can be expressed as the following:

$$Q_1 = \{p_1, p_2, \ldots p_n\}\ Q_2 = \{q_1, q_2, \ldots q_m\} \tag{7}$$

(4) Creating distance matrix $\boldsymbol{D}$: An $(n+1) \times (m+1)$ matrix $\boldsymbol{D}$ is created, where the element D_{ij} is the distance $dis(p_i, q_j)$ between the points p_i and q_j, which can be expressed as the following:

$$D_{ij} = dis(p_i, p_j) = \sqrt{(x_{pi} - x_{qj})^2 + (y_{pi} - y_{qj})^2} \tag{8}$$

(5) Calculating loss matrix $\boldsymbol{M}$: Based on the distance matrix $\boldsymbol{D}$, another $(n+1) \times (m+1)$ matrix $\boldsymbol{M}$ is created. This can be expressed as the following:

$$M_{ij} = \begin{cases} D_{ij} & i = 0, j = 0 \\ D_{ij} + \min\{D_{i-1,j-1}, D_{i,j-1}, D_{i-1,j}\} & 1 \le i \le n, 1 \le j \le m \end{cases} \tag{9}$$

(6) Calculating the distance between sequences Q_1 and Q_2: The distance between sequences Q_1 and Q_2 is the 2-norm of the loss matrix $\boldsymbol{M}$. The smaller the value, the higher the similarity between curves C_1 and C_2.

(7) Solving for the initial positioning location: Using the above method, the curve C_2 that is in highest similarity with the product contour C_1 is extracted. Then, according to the shortest distance in the loss matrix $\boldsymbol{M}$, the points in sequence Q_1 corresponding to those points in set Y are obtained. Finally, by moving these obtained points from Q_1 via the translation vectors recorded in step (2), the positioning point set X is obtained.

In summary, the locator planning method based on the DTW trajectory comparison algorithm is used to compare the projected contour curve C_1 of the product with the

projected curve C_2 of the typical positioning schemes in the knowledge base and extract the optimized version of C_2 that has the most similarity with C_1.

3.3. Layout Planning for the Platform Unit

The paving of the platform unit refers to the combination of platform units according to the length and width (L, W) of a unit and the gap D between connections, as shown in Figure 12. The automatic and rapid completion of this process requires the automatic calculation of the direction and quantity of the platform units according to the determined platform size with a proper planning algorithm. This study designs a paving method for platform units based on dynamic programming.

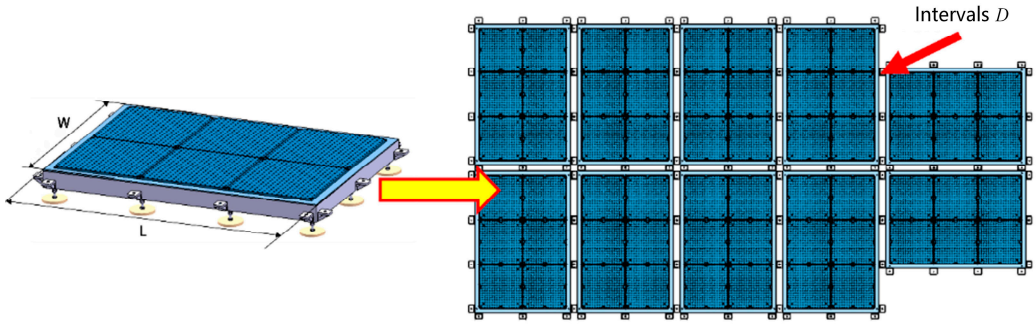


Figure 12. Paving of the platform unit.

Dynamic programming is a decision-making process for optimization by decomposing a complex problem into relatively simple sub-problems, and it is often used for problems with overlapping sub-problems and optimal substructure properties. This study combines this algorithm with a layered paving method to achieve maximum efficiency. The layered paving method refers to several platform units along the same paving direction (longitudinal or transverse) forming a layer, and multiple layers that have different paving directions construct an entire platform. According to the size of the entire platform determined by the product envelope, the initial outer contour of the platform is created, as illustrated in Section 2.3.1. The V and H axes of the outer contour are separately selected as the paving directions of the platform units in layers, and the paving direction of each layer is optimized according to the simulation result. Taking the V-axis as an example, the paving method for one layer based on dynamic programming is firstly introduced as follows.

Firstly, the bottom line of the first layer is obtained, as shown in Figure 13a. Aiming at ensuring that the platform is as regular as possible, the paving direction of all units in each layer is consistent. The platform units are paved along the longitudinal or transverse direction on the bottom line. When the longitudinal direction is selected, the top line of the first layer is the line segment L_{l1} obtained by moving the bottom line upward by the sum of L and D within the initial outer contour, as shown in Figure 13a. Similarly, when the transverse direction is selected, the top line of the first layer is the line segment L_{w1} obtained by moving the bottom line of the first layer upward by the sum of W and D within the initial outer contour.

In order to save costs and ensure the complete coverage of the initial outer contour, the paved units of the first layer should be the fewest and should cover the top line. If the units are paved along the longitudinal direction, the number n_{l1} of platform units is the result of the division of L_{l1} by $L + D$ and is rounded up. This can be expressed by the following:

$$n_{l1} = [L_{l1}/(L + D)] + 1 \tag{10}$$

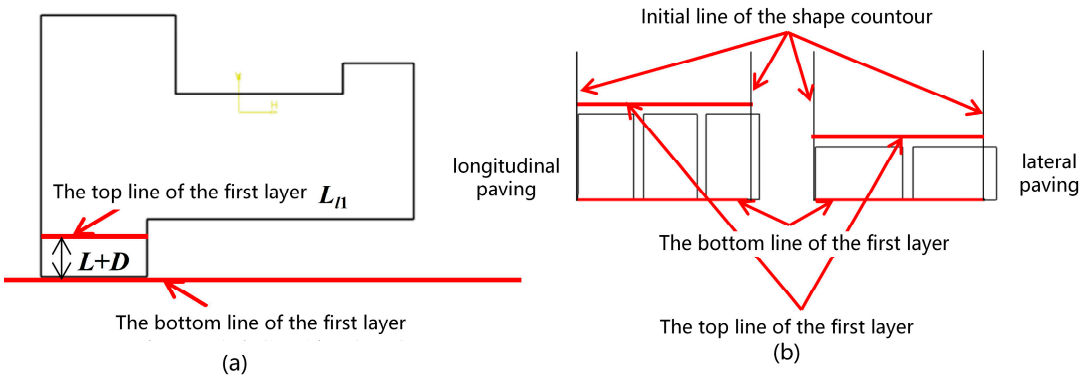


Figure 13. (**a**) Schematic diagram of the bottom and top lines of the first layer; (**b**) schematic diagram of the first layer laid along two directions.

If the platform units are paved along the transverse direction, the number n_{w1} of platform units is the result of the division of L_{w1} by $W + D$ and is rounded up. This can be expressed by the following:

$$n_{w1} = [L_{w1}/(W + D)] + 1 \tag{11}$$

The paving of the first layer of the platform along two directions is shown in Figure 13b.

To ensure the standardization of the design, for adjacent layers, if the top line of the former layer coincides with that of the latter layer after being offset by a certain distance, then the paving methods and quantities of the platform units of these adjacent layers are consistent. As shown in Figure 14, if the n th layer is paved horizontally and its top line coincides with that of the $n + 1$ th layer after being offset upward by $W + D$, then the paving of the $n + 1$ th layer is also along the horizontal direction, and the quantity of units is the same as that in the n th layer. On the contrary, if the top line of the n th layer does not coincide with that of the $n + 1$ th layer after being offset by an arbitrary distance, then there are two choices of the paving direction for the $n + 1$ th layer, and the quantity of units needs to be recalculated according to the new top line of the $n + 1$ layer.

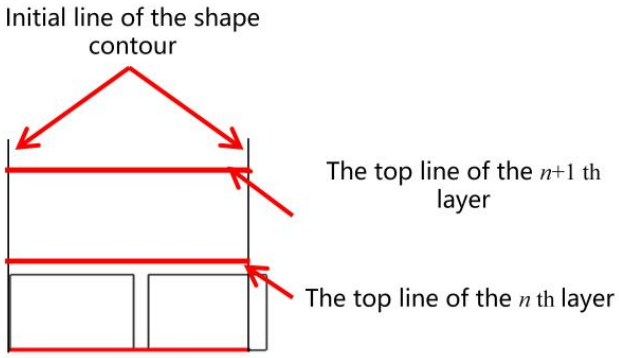


Figure 14. Schematic diagram of the adjacent paving layers.

On the basis of the above method for platform paving in layers, a dynamic programming algorithm is used to solve for the optimized scheme that uses the fewest units to construct the entire platform. The total number of units used is denoted as *Sum*. The whole process of optimization is divided into the following three steps:

(1) The process is divided into different stages.

Boundaries are set to divide the process into different stages when the top line of the previous paving layer does not coincide with that of the next paving layer after being offset.

This means that if the paving direction and unit quantity of a layer need to be redetermined, then the paving of the layer is in a new stage after the previous one.

(2) The paving scheme of each stage is determined.

In general, each stage has two schemes for choices, which are classified according to the paving direction. During the i th stage, the numbers of platform units separately calculated from the paving directions along the longitude and transverse are represented as N_{ij} and $N_{i,j+1}$. Taking the first stage shown in Figure 15 as an example, when the longitudinal direction is chosen, the value for the paved layer during this stage is only one, and the quantity of units in N_{11} is calculated as 3. When the transverse direction is chosen, the value for the paved layer during the first stage is two, and the quantity of units in N_{12} is calculated as 4.

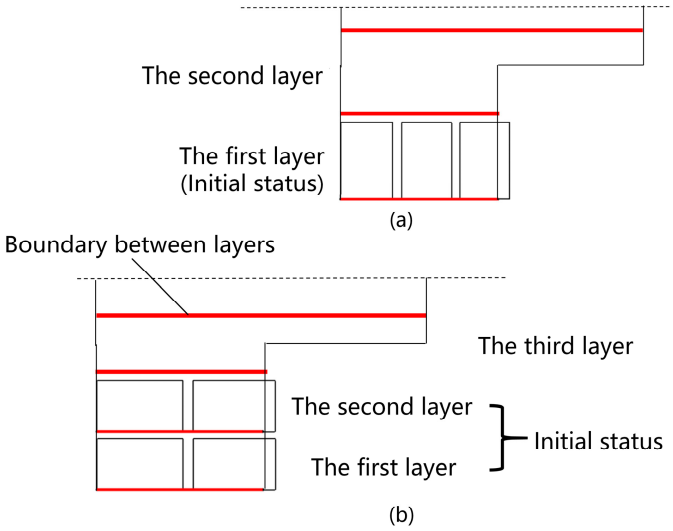


Figure 15. An example of the first paving stage: (**a**) longitudinal paving; (**b**) horizontal paving.

(3) The state transition equation is determined.

Based on the determination of each stage in two paving directions, a paving strategy diagram can be drawn, and one of its examples is shown in Figure 16, where $N[i][j]$ represents the total number of platform units needed for the chosen direction during the i th stage, and j is the ordinal number of the term.

As described previously, the optimal paving strategy involves letting the total number Sum of units reach its minimum value. Let $MINSum_{ij}$ represent the minimum number of platform units needed from node $N[i][j]$ in the i th stage to one of the nodes in the last stage. The corresponding path of $MINSum_{ij}$ from $N[i][j]$ to the last stage is part of the optimal strategic path that will be determined. Then, if the entire paving process contains a total of m stages, the state transition equation can be derived as follows:

$$MINSum_{ij} = \begin{cases} N[i][j] & i = m \\ \min\{N[i+1][2j-1], N[i+1][2j] + N[i][j]\ \} & i \neq m \end{cases} \quad (12)$$

According to the state transition equation, the optimal strategic path is solved by starting from the node with the smallest value in the first stage and reaching the last stage. For the above example, since $N_{11} < N_{12}$, the optimal strategy is the calculation process of solving $MINSum_{11}$, and this can be easily obtained by traversing all of the quantities of units represented by the nodes in the first stage.

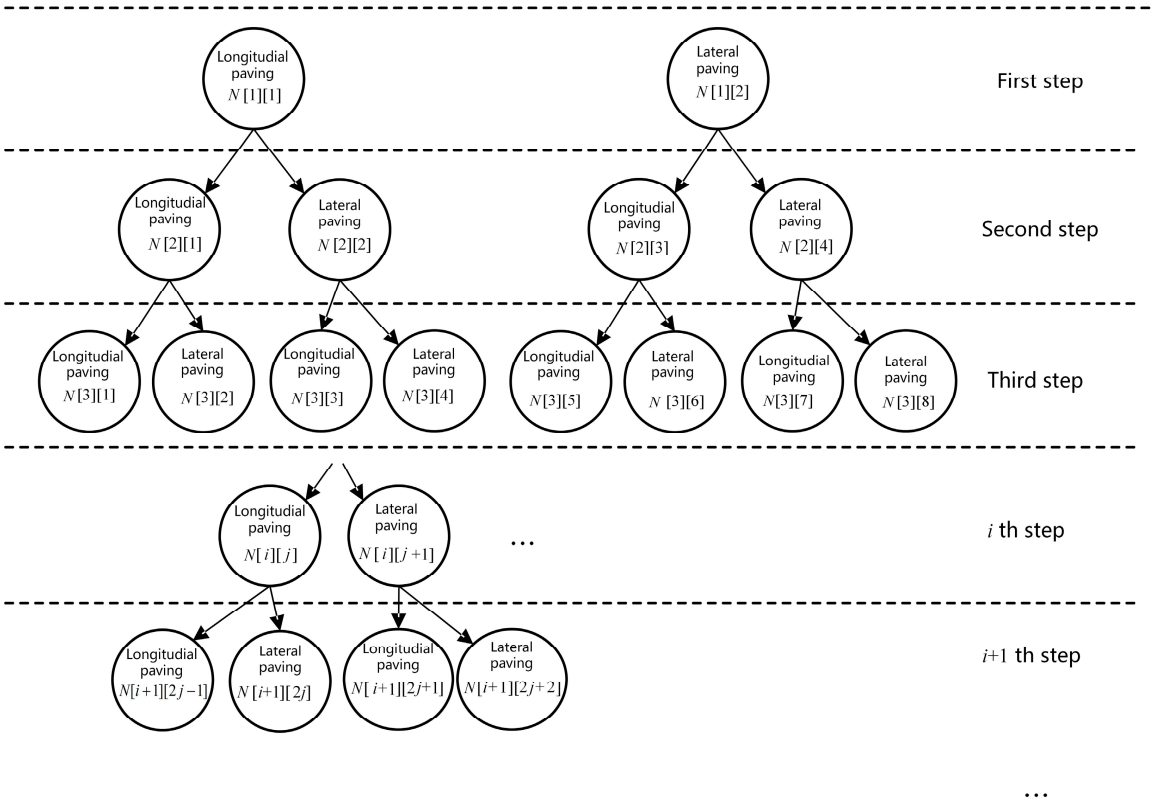


Figure 16. Diagram of the paving strategy.

4. Verification Example

4.1. Planning of the Positioning Layout

The assembly of two types of products was taken as an example for verification. The design of the reconfigurable tooling was completed using software that was developed based on CATIA and contained a function for reconfiguration planning.

Figure 17 shows the geometric features and dimensions of the two products, which are named A and B. Considering their sizes and structural characteristics, product A is assembled in a vertical posture, while product B is assembled in a horizontal posture. For the determinations of the positioning and support during assembly, the outer contours of products A and B are extracted from the top view.

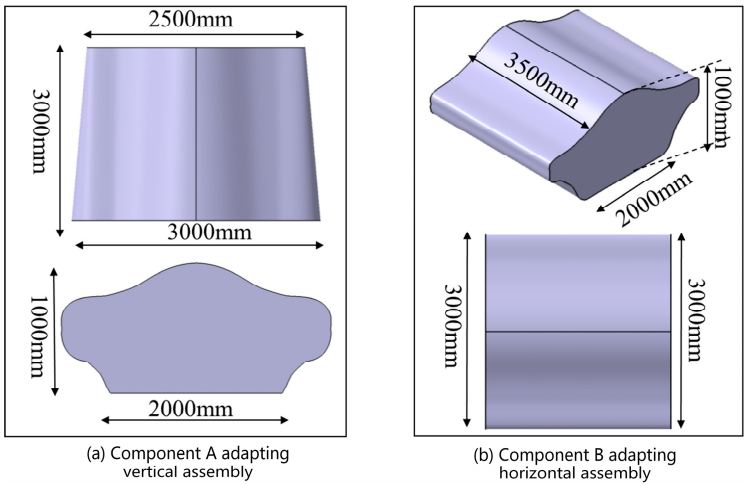


Figure 17. Assembly scheme and process features of components A and B.

Based on the DTW trajectory comparison algorithm, the initial points for the bottom support and positioning during assembly are calculated. The number of initial positioning points is set to 11, and then a comparative calculation is carried out. According to the projection curve *C* of component A's outer contour, the smallest rectangle that can envelop curve *C* on the platform surface (with the platform surface approximated as a horizontal plane) is obtained, and then the midpoint of the rectangle is used as the origin point $\boldsymbol{o}$ to create a local coordinate system: $\boldsymbol{xoy}$. The initial positioning points calculated with the DTW algorithm are projected onto the platform surface to obtain their coordinates within the coordinate system $\boldsymbol{xoy}$. The calculation results are shown in Table 1.

Table 1. Calculation results for the initial positioning points for product A.

Positioning Point	P1	P2	P3	P4	P5	P6	P7	P8	P9	P10	P11
x coordinate	−1325	−535	−297	291	536	1390	1335	1201	60	−1180	−1344
y coordinate	189	492	563	575	512	188	−296	−444	−688	−455	−305

Similarly, based on the DTW trajectory comparison algorithm, the initial positioning points for the horizontal assembly of product B are calculated. The number of positioning points is set to 10, and then the calculation is carried out. The coordinates of these points within the local system defined on the platform plane are shown in Table 2.

Table 2. Calculation results for the initial positioning points for product B.

Positioning Point	P1	P2	P3	P4	P5	P6	P7	P8	P9	P10
x coordinate	8255	8233	9745	10,958	10,857	10,844	10,962	9771	8211	8269
y coordinate	−1019	−1798	−1775	−1764	−622	645	1799	1755	1760	1000

The determined positioning points for products A and B from the top view are shown in Figure 18a, and the time consumed by the planning process for the positioning points based on the DTW trajectory comparison algorithm is shown in Figure 18b. The time consumed is only a few seconds, thus validating the efficiency of the planning of the positioning layout.

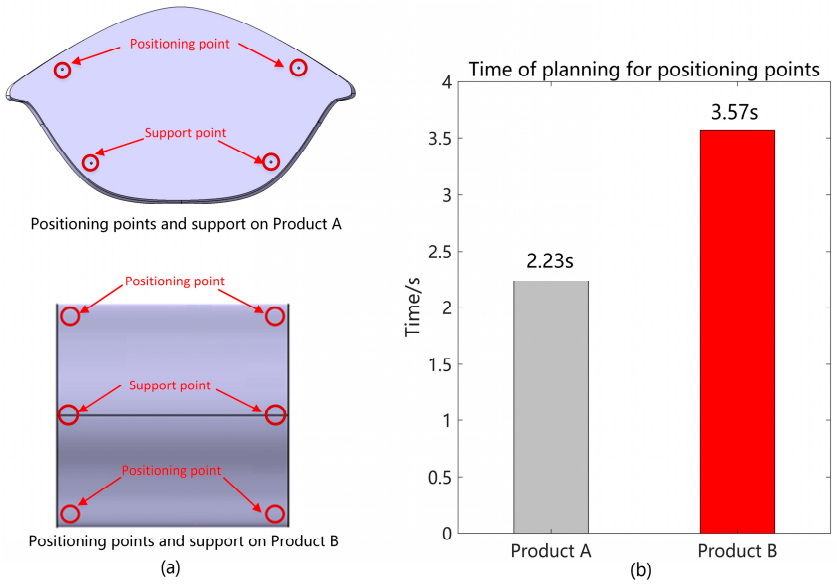


Figure 18. (**a**) The planning results for the positioning and support points for products A and B; (**b**) the time consumed by the planning process.

The stress distributions of products A and B under gravity and the layouts of the support planned by the DTW algorithm and personnel are shown in Figure 19. As demonstrated by the comparisons between the stress distributions resulting from the support layouts planned by the algorithm and personnel, the stress of products A and B under manually planned support is greater and more concentrated, since the distributions of support and positioning points planned by the algorithm are more dispersed and more appropriate than those planned manually using human experience. Benefiting from the integration and analysis of multiple layout schemes in the database, the DTW algorithm can output an optimal positioning scheme and support layout that is best suited for the current product.

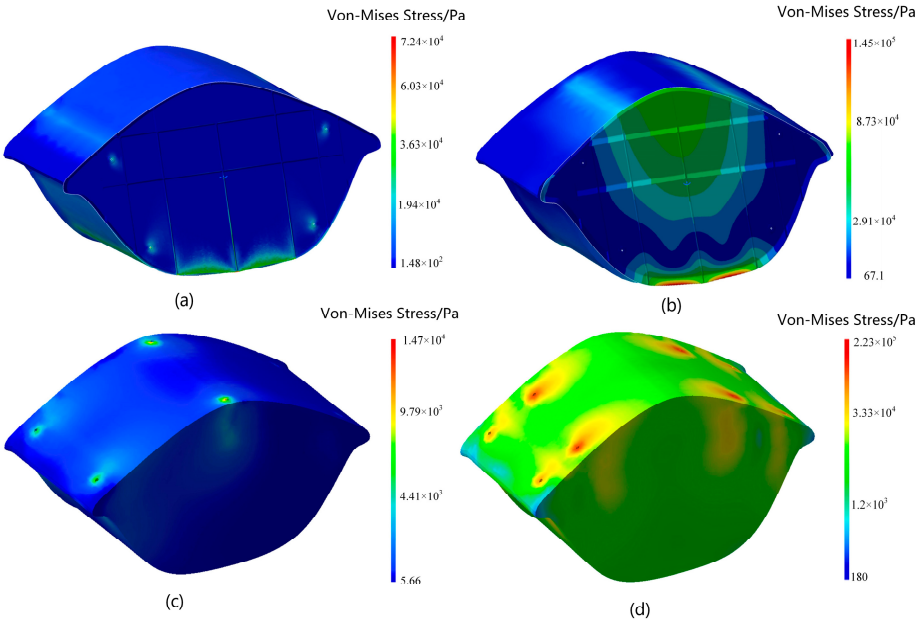


Figure 19. The stress distributions of products A and B under gravity and different layouts of supports: (**a**) product A under the support layout planned using the DTW algorithm; (**b**) product A under the manually planned support layout; (**c**) product B under the support layout planned using the DTW algorithm; (**d**) product B under the manually planned support layout.

4.2. Rapid Design of Reconfigurable Tooling

Firstly, the projection of product A is extracted onto the platform plane, as shown in Figure 20a. The points on the projection curve are used as inputs, the planning algorithm is run based on dynamic programming, and the optimized scheme of a 3 × 3 layout for the paving units of the platform is provided as an output. Then, the platform planning module of the design software is run to carry out the rapid assembly of digital models. The user specifies the *X*/*Y* direction for the platform's installation in the digital environment and inputs the number of units in the two directions. The software automatically inputs models of platform units with assembly constraints. When the platform units are assembled, the software automatically starts the rapid assembly of the remaining parts, such as pedals and connecting pieces, to complete the entire process, as shown in Figure 20b.

Then, the initial positioning points calculated using the planning algorithm are input into the current digital model. The user can design the installation positions of columns according to these points and then initiate the corresponding module in the software, where they can select the types of columns and their installation positions by clicking the points on the platform model as shown by the red circles in Figure 21a. The column models can be rapidly input, as shown in Figure 21b. Finally, the user can enable the installation module of the locator to achieve the rapid assembly of the beam and sliding rail units on the column

through a similar operation. The final design model in digital space is shown in Figure 21c. The time taken by a group of processing personnel to complete the whole design process is shown in Figure 21d. As shown in Figure 21d, the design time was only around 10 min at most, and it was far less than that of the traditional design process, which usually requires several days.

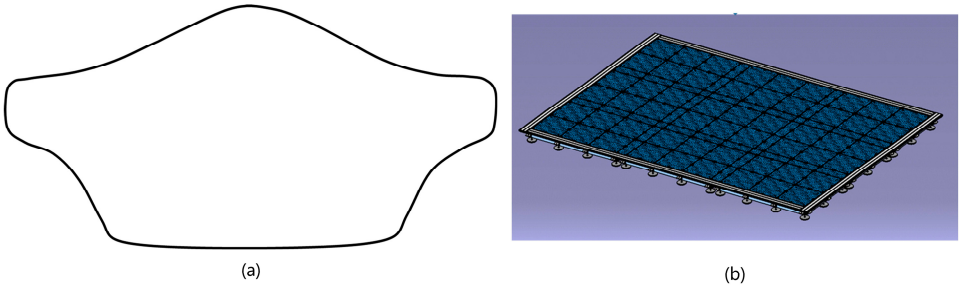


Figure 20. (**a**) Horizontal projection of product A; (**b**) paving results of platform units.

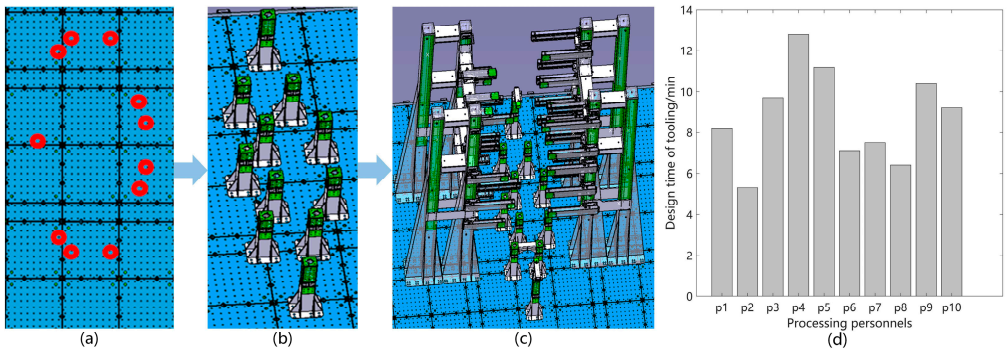


Figure 21. Design process of the assembly tooling for product A in a vertical posture: (**a**) selection of column installation positions; (**b**) importing a column model; (**c**) importing beam and sliding rail units; (**d**) time taken for the design process to be completed by 10 processing personnel.

Similarly, the projection of product B in a horizontal posture is extracted on the platform plane. Then, the planning algorithm runs and outputs the scheme of platform paving, for which a 3 × 3 layout is also adopted, and the unit models are automatically input to form the platform. Finally, the column and locator models are imported and rapidly assembled according to the positioning points planned for product B. The process and result of the tooling design for the horizontal assembly of product B are shown in Figure 22a–c. The time taken by 10 personnel to complete the design process is shown in Figure 22d. As in the assembly tooling of product A, the process of tooling design for product B only takes 10 min, which is notably less than the several days required for a traditional design process.

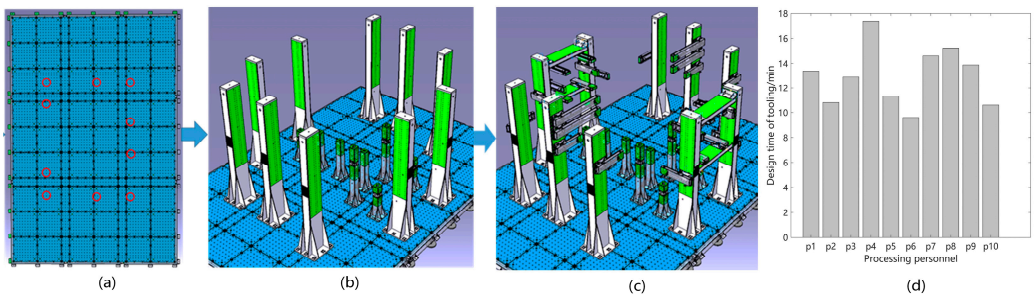


Figure 22. Design process and result of the assembly tooling for product B: (**a**) selection of column positions; (**b**) importing a column model; (**c**) importing beams and sliding rails; (**d**) time consumed by the design process when completed by 10 personnel.

4.3. Monitoring System for Assembly Tooling

On the basis of modular design and reconfiguration planning technology, tooling integrated with multi-source sensors is manufactured and applied to assemble a practical type of aircraft fuselage. As shown in Figure 23a, three-dimensional force sensors and fiber Bragg gratings are arranged on locator beams to separately sense their loads and deformation in real time. In addition, temperature and vibration sensors are installed on the columns and beams to detect the thermal deformation and mechanical vibration of the tooling structure. Details of the sensor layout are shown in Figure 23b. More detailed information on the use of fiber Bragg gratings and deformation sensors can be found in our previous work [10].

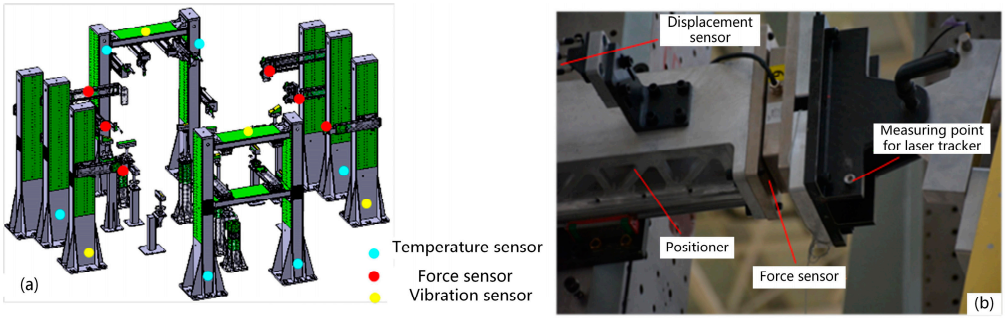


Figure 23. (**a**) Schematic diagram of the sensor layout; (**b**) details of the sensor layout.

An online monitoring software system containing information on the vibrations, clamping force, and environmental temperature of the tooling structure was developed to provide warnings about stress and positioning errors during the assembly process. The monitoring software interface developed in this study is shown in Figure 24. In this interface, the deformation and temperature distributions of the tooling structure are intuitively presented through a three-dimensional model with a nephogram, and the current clamping force, temperature, and vibration are presented using waveforms on the right side of the interface, providing a good visualization of the online service state of the tooling. When the measures exceed their thresholds, the system issues a warning and makes recordings. This provides an example for the realization of intelligent assembly based on reconfigurable tooling.

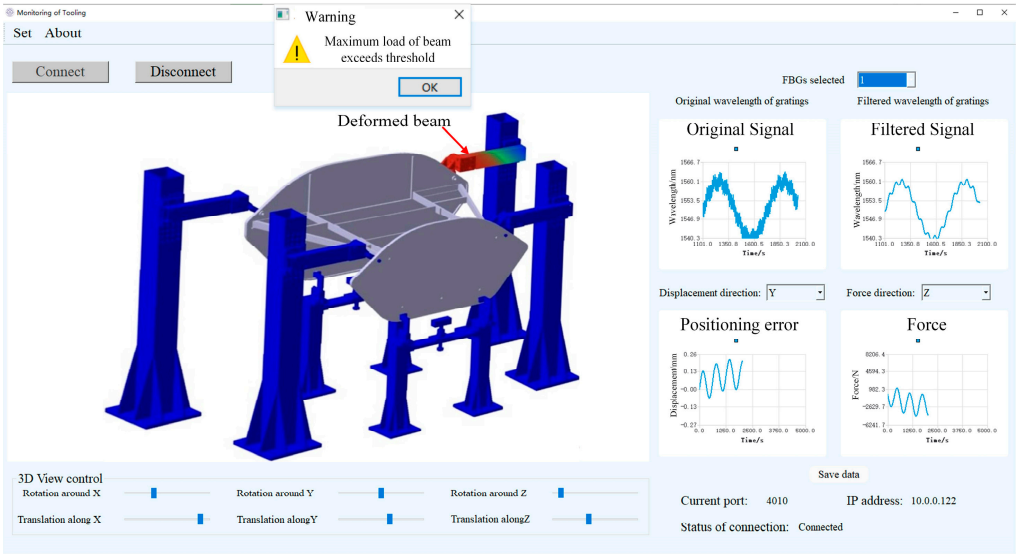


Figure 24. Interface of the monitoring system for reconfigurable tooling.

5. Conclusions

This study investigated the modular design of aircraft assembly tooling, as well as how to optimize its configuration, to enhance the generality of designs and their ability to rapidly respond to product changes. The main conclusions are as follows:

(1) In terms of the modular structure design, the concept of functional elements is proposed, and a diagram revealing the relationships between functional elements of all tooling parts is established. Based on this diagram, the similarity between structures is defined and calculated. The tooling structure is divided and reorganized into modules according to similarity, and a detailed design of the modules is presented using three typical structures, namely, platforms, columns, and locators. Modularization and serialization make the structures lightweight and simplified, enhancing the design efficiency and openness of the assembly space while guaranteeing structural rigidity and stability.

(2) In terms of reconfiguration technology, a parametric representation of modular structures is proposed, and a knowledge base is constructed to achieve efficient transmission and storage of structural information. By using the parametric information of structures, the locator layout and platform configuration are separately optimized based on the DTW trajectory comparison and dynamic programming algorithms, thus allowing for the rapid reconfiguration of tooling. The usage of releasable screws for the adjustment of structures guarantees both adaptability and stability.

Reconfigurable tooling is built and successfully applied to the assembly of a practical type of aircraft fuselage. A system for monitoring multi-source information, including structural vibrations, environmental temperature, and clamping force, is developed, thus enabling early warnings about assembly stress and positioning errors. This engineering verification provides a paradigm for the serialization, modularization, and intellectualization of aircraft assembly tooling.

Author Contributions: Conceptualization, Z.S. and J.H.; methodology, Z.S.; software, C.L.; validation, Z.S.; formal analysis, C.L.; resources, Z.S.; writing—original draft preparation, C.L.; writing—review and editing, J.H., X.S. and H.W.; supervision, W.T.; project administration, W.T. All authors have read and agreed to the published version of the manuscript.

Funding: The work reported herein was financially supported by the National Key Research and Development Program of China (Grant No. 2019YFB1707403), Natural Science Foundation of Jiangsu Province (BK20202007), and Fundamental Research Funds for the Central Universities (Grant No. NT2024013).

Data Availability Statement: Data will be made available upon request from the corresponding author.

Conflicts of Interest: Author Zhanghu Shi was employed by the company Aviation Industry Chengdu Aircraft Industry (Group) Co., Ltd. The remaining authors declare that the research was conducted in the absence of any commercial or financial relationships that could be construed as a potential conflict of interest. The funders had no role in the design of the study, the collection, analyses, or interpretation of data; the writing of the manuscript; or the decision to publish the results.

References

1. Grieves, M. *Virtually Perfect: Driving Innovative and Lean Products Through Product Lifecycle Management*; USA Space Coast Press: Merritt Island, FL, USA, 2011.
2. Hu, F.; Li, D. Process Planning and Simulation Strategies for Perimeter Milling of Thin-walled Flexible Parts Held by Reconfigurable Fixturing System. In Proceedings of the Third International Conference on Measuring Technology and Mechatronics Automation, Shangshai, China, 6–7 January 2011; pp. 922–926.
3. Xie, F.; Liu, X.J.; You, Z.; Wang, J. Type synthesis of 2T1R-type parallel kinematic mechanisms and the application in manufacturing. *Robot. Comput. Integr. Manuf.* **2014**, *30*, 1–10. [CrossRef]

4. Bi, Z.M.; Lang, S.Y.T.; Verner, M.; Orban, P. Development of reconfigurable machines. *Int. J. Adv. Manuf. Technol.* **2008**, *39*, 1227–1251. [CrossRef]
5. Naing, S. Feature based Design for Jig-Less Assembly. Ph.D. Thesis, Crandfield University, Bedfordshire, UK, 2004.
6. Schwake, K.; Wulfsberg, J. Robot-based system for handling of aircraft shell parts. *Procedia Cirp* **2014**, *23*, 104–109. [CrossRef]
7. Zhu, Y.G.; Huang, X.; Li, S.G. A novel six degrees-of-freedom parallel manipulator for aircraft fuselage assemble and its trajectory planning. *J. Chin. Inst. Eng.* **2015**, *38*, 928–937. [CrossRef]
8. Esser, M.; Vette, M. Reconfigurable handling systems as an enabler for large components in mass customized production. *J. Intell. Manuf.* **2013**, *24*, 977–990.
9. Tao, F.; Cheng, Y.; Zhang, L.; Nee, A.Y.C. Advanced manufacturing systems: Socialization characteristics and trends. *J. Intell. Manuf.* **2015**, *7*, 1079–1094. [CrossRef]
10. Li, C.; Hu, J.; Kang, R.; Yang, Y.; Jin, J.; Tian, W. Structural deformation and clamping force monitoring of reconfigurable tooling motivated by strain data in aircraft assembly. *Smart Mater. Struct.* **2024**, *33*, 055046. [CrossRef]
11. Muller, R.; Esser, M.; Mbarek, T.; Biyiklioglu, N.; Quinders, S. *Development of Modular Low-Cost Automation Systems for Aircraft Assembly*; SAE Technical Papers; SAE: Warrendale, PA, USA, 2011.
12. Schneider, T. Innovative approach for modular and flexible positioning systems for large aircraft assembly. In Proceedings of the SAE 2015 AeroTech Congress & Exhibition, Washington, DC, USA, 22–24 September 2015.
13. Kihlman, H. Affordable Automation for Airframe Assembly Development of Key Enabling Technologies. Ph.D. Thesis, Linkoping University, Linkoping, Sweden, 2005.
14. Basile, F.; Caccavale, F.; Chiacchio, P.; Coppola, J.; Marino, A.; Gerbasio, D. Automated synthesis of hybrid Petri net models for robotic cells in the aircraft industry. *Control. Eng. Pract.* **2014**, *31*, 35–49. [CrossRef]
15. Jonsson, M.; Ossbahr, G. Aspects of reconfigurable and flexible fixtures. *Prod. Eng.* **2010**, *4*, 333–339. [CrossRef]
16. Löchte, C.; Dietrich, F.; Raatz, A. *A Parallel Kinematic Concept Targeting at More Accurate Assembly of Aircraft Sections*; Springer: Berlin/Heidelberg, Germany, 2011; pp. 142–151.
17. Prause, I.; Mbarek, T.; Corves, B. Increasing the stiffness of a 3-PUU parallel kinematic positioning device for high payloads by modifying the leg configuration. In Proceedings of the IFToMM Workshop on Fundamental Issues and Future Research Directions for Parallel Mechanisms and Manipulators, Tianjin, China, 7–8 July 2014.
18. Jefferson, T.; Crossley, R.; Smith, T. *Review of Reconfigurable Assembly Systems Technologies for Cost Effective Wing Structure Assembly*; SAE Technical Papers; SAE: Warrendale, PA, USA, 2013.
19. Jonsson, M.; Kihlman, H.; Ossbahr, G. Coordinate controlled fixturing for affordable reconfigurable tooling. In Proceedings of the 2nd Conference on Assembly Technologies and Systems, Tianjin, China, 10–12 May 2008; pp. 1–11.
20. Kihlman, H. *Flexapods-Flexible Tooling at SAAB for Building the NEURON Aircraft*; SAE Technical Papers; SAE: Warrendale, PA, USA, 2010.
21. Xiong, L.; Molfino, R.; Zoppi, M. Fixture layout optimization for flexible aerospace parts based on self-reconfigurable swarm intelligent fixture system. *Int. J. Adv. Manuf. Technol.* **2013**, *66*, 1305–1313. [CrossRef]
22. Mannheim, T.; Riedel, M.; Hüsing, M.; Corves, B. A new way of grasping: PARAGRIP—The fusion of gripper and robot. *Grasping Robot.* **2013**, 433–464.
23. Molfino, R.; Zoppi, M.; Zlatanov, D. Reconfigurable swarm fixtures. In Proceedings of the Asme/Iftomm International Conference on Reconfigurable Mechanisms and Robots, London, UK, 22–24 June 2009; IEEE: Piscataway, NJ, USA, 2009; pp. 730–735.
24. Ramirez, J.; Wollnack, J. Flexible automated assembly systems for large CFRP-structures. *Procedia Technol.* **2014**, *15*, 447–455. [CrossRef]
25. Erdema, I.; Helgosson, P.; Kihlman, H. Development of Automated Flexible Tooling as Enabler in Wing Box Assembly. *Procedia CIRP* **2016**, *44*, 233–238. [CrossRef]

Disclaimer/Publisher's Note: The statements, opinions and data contained in all publications are solely those of the individual author(s) and contributor(s) and not of MDPI and/or the editor(s). MDPI and/or the editor(s) disclaim responsibility for any injury to people or property resulting from any ideas, methods, instructions or products referred to in the content.